# Electric Behavior Characterization of Lithium Iron Phosphate Batteries as a Function of Operating Temperature

Ibrahima Touré[1,2], Joselyn Stephane Menye[1], Alireza Payman[1], Mamadou-Baïlo Camara[1,2] and Brayima Dakyo[1]
[1]GREAH-Laboratory, University of Le Havre Normandie; [2]Research Laboratory in Applied Sciences of Mamou (LaReSA)
Le Havre, France; Mamou, Guinea
ibrahima.toure@etu.univ-lehavre.fr (I.T.); joselyn-stephane.menye@univ-lehavre.fr (J-S.M); alireza.payman@univ-lehavre.fr (A.P.); mamadou-bailo.camara@univ-lehavre.fr (M.B.C.); brayima.dakyo@univ-lehavre.fr (B.D.)

***Abstract*— This paper presents evaluation of temperature variations on electric behavior of iron phosphate batteries. Indeed, the aim of this study is to show the effects of operating temperature on the series resistances and the capacities of the electrical model. More precisely, the paper's contribution focuses on the study of the degradation of lithium iron phosphate batteries parameters as a function of the temperature for increasing and decreasing phases of temperature. To determine the batteries, charge and discharge capacities and series resistance, experimental characterization is carried out by using different predetermined protocols. That leads to determination of electrical model parameters under various temperature conditions.**

***Keywords*— *Lithium iron phosphate batteries; Electrical characterization; Temperature; Series resistance; Battery capacity.***

## I. INTRODUCTION

The energy crisis underlies many of the challenges and opportunities facing the world today. All energy production sources have drawbacks, including air pollution, accidents, and greenhouse gas emissions [1]. Renewable energy sources are emerging as serious contenders for fossil fuel substitution, helping to reduce greenhouse gas emissions. In a global context marked by ambitious renewable energy targets, their deployment has intensified across industrial, commercial, public, and residential sectors [2][3]. However, the intermittent nature of these resources, heavily dependent on weather conditions and changing seasons, underscores the crucial role of efficient energy storage systems in promoting the widespread adoption of renewable energy technologies in homes [2]. Storage systems now play a central role in integrating renewable energy sources into the traditional energy market while ensuring a stable and reliable power supply in smart grids [4].

Of all energy storage technologies, lithium batteries (LIBs) are the most widely used in industry today. They serve a broad range of applications, from smartphones to aerospace and electric vehicles [5]-[7]. Among the various types, the lithium iron phosphate (LiFePO4, LFP) battery is particularly popular due to its thermal stability and low cost compared to other technologies.

Despite their central role, LIBs face several limitations and constraints. Numerous studies have demonstrated that temperature plays a critical role in the aging and failure of LIBs [8][9]. These effects are often characterized by failures such as thermal runaway and aging, which are based on variations in the components' capacitance and internal resistances. Many studies have evaluated the impact of operating temperature on battery series resistances and capacity, primarily focusing on test protocols involving charge and discharge cycles.

In the work conducted by Yue et al. [10], tests were carried out using three types of batteries over a wide temperature range, from -50°C to 50°C. The results indicate that ohmic resistance increases significantly as the temperature decreases, particularly below -30°C, a phenomenon attributed to the increased viscosity of the electrolyte. Among the technologies evaluated, LFP batteries exhibited the lowest resistance and were the least sensitive to temperature variations.

In another study [11], the authors focused on characterizing and modeling the aging of LFP batteries under the combined effects of temperature and DC current ripple frequency. The tests were based on experimental data covering 4,800 cycles, with frequency variations from 50 to 500 mHz and temperature variations from 10 to 80°C. The results reveal that series resistance increases with frequency but decreases with rising temperature. Conversely, energy capacity increases with both temperature and frequency.

In [12], Ahmed et al. studied two types of batteries at different temperatures, demonstrating that cell resistance increases significantly at low temperatures. Their analysis also revealed that the interfacial resistance of the anode is nearly twice that of the cathode, highlighting its predominant role in ohmic losses.

In [13], the research investigates the influence of cathode material and temperature on the discharge capacity of LIBs. They found that as temperature rises, electrolytic activity changes, leading to an initial increase followed by a decrease in discharge capacity. For LFP technology, correlations have been established between capacity, internal resistance, ambient temperature, and state of charge. At extreme temperatures ($T \geq 50°C$ or $T \leq 20°C$), capacity decreases. However, as long as the temperature remains above 0°C, capacity stays above 93.4%, before dropping significantly below this threshold. Previous work [14][15] has highlighted the contribution of temperature to battery aging, with its effects often studied alongside other factors, such as charge/discharge current or State of Charge (SoC).

In this paper, we propose an analysis focused exclusively on the influence of temperature on ohmic resistance as well as on charge and discharge capacities. A comparative approach is adopted between two thermal profiles: one with increasing temperature and the other with decreasing temperature.

The structure of this paper is designed to present the experimental approach and the results obtained in a progressive and methodical manner. Section II details the experimental setup and the general conditions under which the

tests were conducted, ensuring the reproducibility and reliability of the measurements. Section III outlines the methodology used to estimate the main electrical parameters of LIBs, specifically series resistance and capacity, from the experimental data. Section IV presents the results obtained and provides an in-depth analysis of the observed effects, highlighting the correlations between the measured parameters and the test conditions. Finally, Section V summarizes the main conclusions of the study and suggests perspectives for future work in the modeling and characterization of electrochemical storage systems.

## II. Description of Experimental Setup and General Tests Conditions

### A. Description of the test environment:

The experimental test bench used in this study is illustrated in Figure 1 and comprises a climatic chamber (model ARS-0220), a battery cycler (BT2000/ARBIN BT-ML) and a real-time control system (MITS-PRO). The NI cDAQ-9174 module acquires and records the temperature, the batteries currents and the cells terminal voltages.

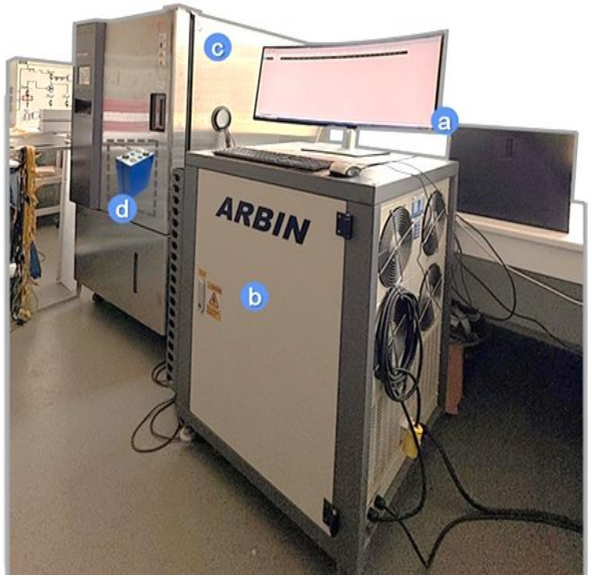


Figure 1. Test bench: (a) Computer running MITS-Pro software, (b) Battery cycler, (c) Climatic chamber (d) Battery pack.

The batteries are subjected to thermal stress during the charging and discharging phases, imposed by a 120-liter environmental chamber with an operating range from -75°C to 180°C. The test bench is controlled via an RS232 interface, allowing for synchronization of events between the BT2000 cycler and the environmental chamber.

Tests were conducted on LF50K cells (3.2V, 50Ah), which have a nominal capacity of 50 Ah. The proposed analysis method is generic and can be adapted to other battery technologies without modification of the experimental protocol, provided the temperature ranges recommended by manufacturers are adhered to.

Tests consist of periodic voltage cycles applied to the batteries, ranging from 2.5 V to 3.5 V and vice versa, under the influence of either fluctuating or constant DC current. These charge and discharge cycles are continuously applied, with no interruptions between different phases.

To ensure accurate estimation of the battery's capacity and its series resistance, the measurements are carried out according to the following protocols:

- Temperatures are measured using high-precision sensors (error $\leq \pm 0.1\%$).
- Voltages are measured directly at the cell terminals, thus avoiding disturbances induced by power cables.

### B. Test protocol

It is crucial to design an accurate test protocol; otherwise, incorrect results may arise. In our study, we developed a characterization algorithm to determine the battery's ampere-hour capacity (Q[Ah]) and series resistance. To ensure that the tests are conducted properly and that the correct parameters are accurately collected, we designed an algorithm that incorporates all elements of the protocol. This algorithm is tailored to perform two types of tests:

1) A Constant Current/Constant Voltage (CCCV) charging method to charge and discharge the batteries.
2) In the same program, a second test allows us to determine the series resistance.

Both algorithm tests were implemented through MITS-PRO, an ARBIN Group data acquisition device used as a communication interface, as shown in Figure 1. Measurements are performed with a sampling time of one point per second for the capacity and one point per 0.001 second for the series resistance.

The characterization protocol was studied over an operating temperature range of [-5°C to 55°C] with a charging current of 32 A and a discharging current of -32 A. The two experiments were conducted as follows:

First, the battery is subjected to the test temperature for one hour to allow it to equilibrate with the temperature of the climatic chamber. It is then charged with a constant positive current until the voltage at its terminals reaches the maximum set voltage of 3.55 V, which has been established for both testing purposes and the safety of the module.

Before discharging, the battery is allowed to rest for 30 seconds. A negative current is then applied to discharge the battery until its voltage reaches 2.5 V, the minimum test voltage. At the end of the characterization test, a rest period of 2 hours is set to allow the battery voltage to stabilize. This stabilization period enables us to determine the capacity and resistance of the electrolyte, which are essential for calculating the time constant. Figure 2 provides an illustration of the general protocol of the tests.

As illustrated in Figure 2 and in accordance with the protocol defined in the test algorithm, three distinct phases can be identified, each corresponding to a specific stage in the battery characterization process.

**Phase A** represents the thermal stabilization period. During this phase, the battery is placed in the climate chamber and maintained at the set temperature for a sufficient duration to ensure thermal homogeneity within the cell. In our protocol, this duration is set to one hour, allowing the battery to reach thermal equilibrium with the environment, thereby guaranteeing the reliability of subsequent measurements.

**Phase B** corresponds to a complete battery charge/discharge cycle. The exact sequence (charge followed by discharge or vice versa) is determined by the algorithm's internal logic. The total duration of this cycle is highly dependent on ambient temperature, as the electrochemical properties of the battery, such as capacity and internal

resistance, vary significantly with temperature. This step is essential for assessing the battery's energy behavior under different operating conditions.

**Phase C** is dedicated to determining the battery's series resistance. Unlike the previous phase, this stage does not require a long-term test. It relies on the application of a constant charging current for a short period, followed by a rest phase. In our study, a constant current was applied for 10 minutes, followed by a 5-minute rest period between stages. This method allows us to measure series resistance efficiently and accurately, without placing excessive strain on the battery.

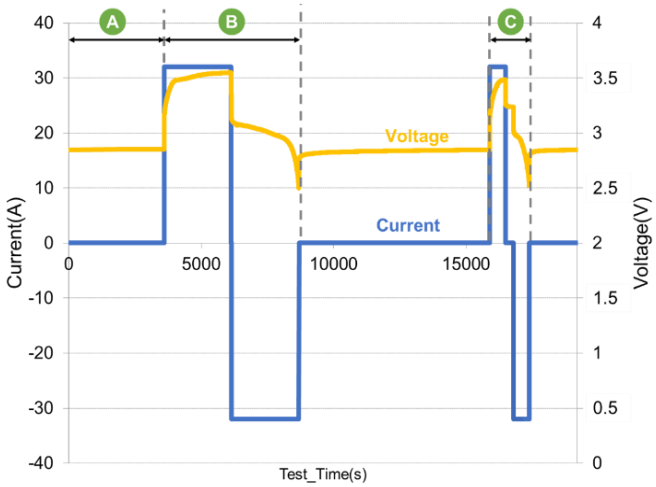


Figure 2. General protocol of the tests.

The sequence of these three phases constitutes the characterization protocol for obtaining the parameters needed to analyze the battery's dynamic behavior.

To determine series resistance, a short-term test was carried out. A constant charging current of 32 A was first applied for a period of 10 minutes. This was followed by a rest period of 5 minutes, before reversing the current to carry out the discharge phase under the same conditions.

## III. CALCULATION OF BATTERY ELECTRICAL PARAMETERS

### A. Behavior model of the battery

Numerous battery models have been proposed in the literature to simulate their dynamic behavior. Most of these models are based on equivalent fixed-parameter electrical circuits, typically composed of constant resistances and capacitances [11][14]. However, such models may be insufficient to accurately represent the actual behavior of batteries, particularly when their characteristics—such as internal resistance, capacity, or SoC—vary over time.

A more realistic model of battery dynamic behavior can be achieved by considering the dependence of these parameters on SoC, as illustrated in Figure 3. Unfortunately, most existing models neglect the evolution of these parameters as a function of temperature during charge and discharge cycles, which limits their accuracy during prolonged simulations or under variable stress conditions.

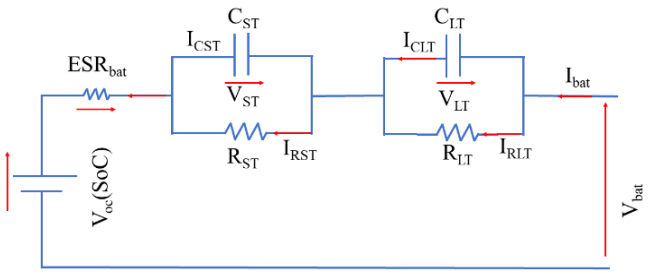


Figure 3. Basic model of the LFP-battery.

The time constants $R_{ST}C_{ST}$ and $R_{LT}C_{LT}$ are estimated based on a detailed analysis of the transient evolution of the battery terminal voltage, conducted immediately after the end of a charging phase or at the very beginning of a discharging phase. This approach accurately captures the dynamic response of the battery under these specific conditions, highlighting the resistive and capacitive components associated with various internal electrochemical phenomena [16][17].

### B. Battery's parameters identification

To determine the parameters of the batteries, it is first necessary to extract the data recorded by the ARBIN system's acquisition software. Among the collected data, a column indicating capacity allows for the direct identification of the batteries' capacity in the table provided by the software. This section presents the method for calculating series resistance from experimental data (current and voltage) obtained during charging and discharging operations.

If the battery does not exhibit hysteresis behavior, the series resistance can be estimated based solely on the experimental data from charging, as the series resistance during discharging will be identical to that obtained during charging. To estimate series resistance from the charging operations, the experimental voltage and current data shown in Figure 4, combined with Equation 1, are used.

Conversely, if the battery exhibits hysteresis behavior, the series resistance must be estimated separately using the charge and discharge data presented in Figures 4 and 5, respectively. Thus, the voltage drops obtained from these figures, noted $\Delta V_{RC}$ and $\Delta V_{RD}$, respectively, can be integrated into Equation 1 to calculate the series resistance corresponding to the battery's charge and discharge phases. The series resistance calculated during charging and discharging operations with a constant current of ±50 A for each temperature is shown in Figures 4 and 5.

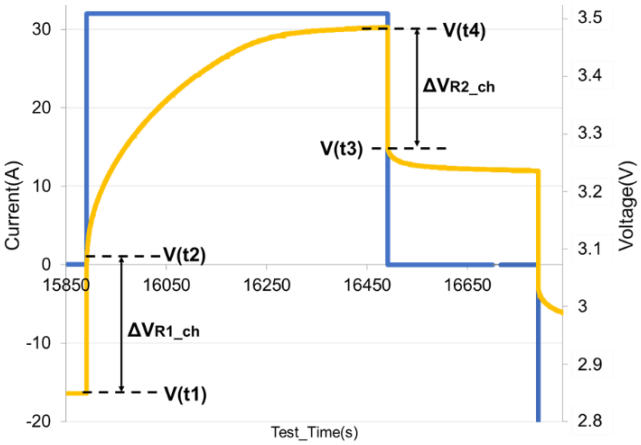


Figure 4. Voltage and current obtained during a charge operation with a constant current of $I_{bat}$ = 50A.

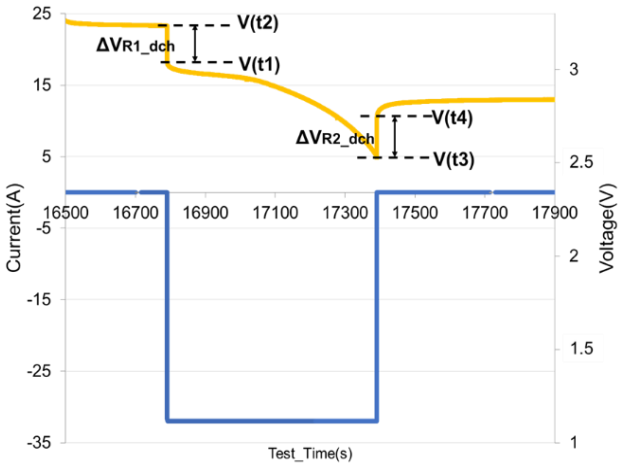


Figure 5. Voltage and current obtained during a discharge operation with a constant current of $I_{bat}$ = -50A.

$$R_i = \begin{cases} R_C = \frac{\Delta V_{RC}}{I_{bat}} & if \ I_{bat} > 0 \\ R_D = \frac{\Delta V_{RD}}{I_{bat}} & if \ I_{bat} < 0 \end{cases} \quad (1)$$

Capacity identification is based on experimental battery voltage and current data, as a function of charging or discharging time. In order to consider into account any differences in parameters between charging and discharging phases, parameter identification must be separately carried out for each operating mode. Figure 6 illustrates a single charge case based on experimental data obtained by measuring voltage, current and response time.

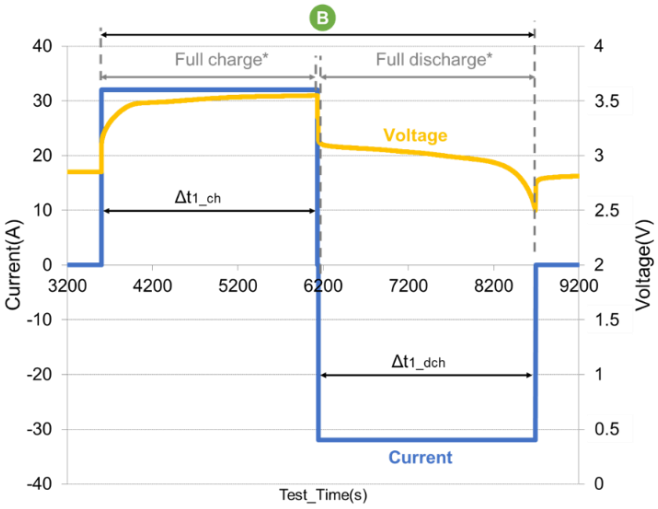


Figure 6. Calculation curve for load capacity/discharge

Battery capacities during charging $Q_{cell\_ch}$ and discharging $Q_{cell\_di}$ are determined using Equation 2.

$$Q_{cell_{ch/di}} \approx \int_{\tau_1}^{\tau_2} I_{bat}.dt \quad (2)$$

Where $\tau_1$ corresponds to the start time of charging/discharging, and $\tau_2$ to the final time of this operation.

## IV. Results and Discussion

After identifying capacity values at different temperatures, a comparative analysis was carried out to assess the thermal effect on the battery's electrochemical behavior. Figure 7 illustrates the evolution of capacities in charge and discharge, as a function of the temperature, considered in both increasing and decreasing scenario. Observation of the curves reveals a tendency for increasing the capacity as temperature rises. This behavior can be explained by improved electrochemical kinetics. This trend is clearly visible in Figure 7, which shows that the capacity extracted is higher at higher temperatures, whether charging or discharging. Conversely, a decrease in temperature is accompanied by a significant drop in measured capacities, reflecting a marked thermal sensitivity of battery's performance.

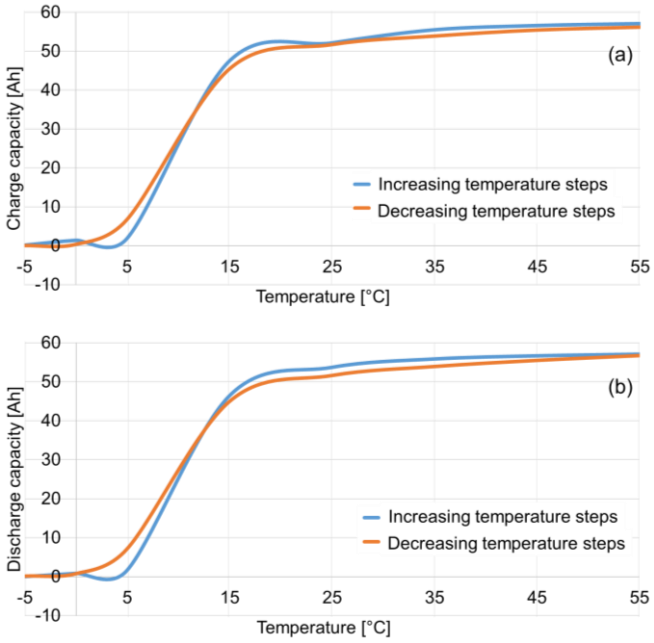


Figure 7. Battery charge and discharge capacity at rising and falling temperatures.

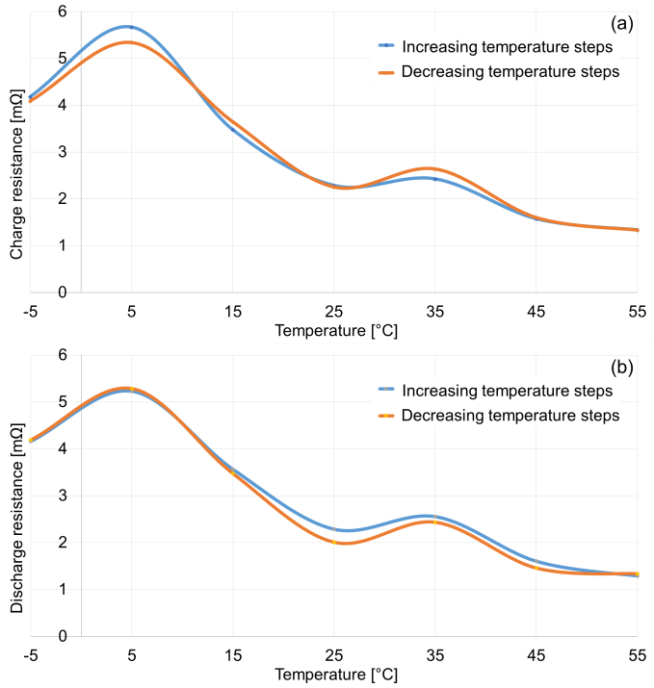


Figure 8. Battery charge and discharge series resistance at rising and falling temperatures

The carried-out calculations identify two values for series resistance, corresponding to the charging and the discharging phases, under the same temperature conditions as those used

in the previous test. The analysis of the results, illustrated in Figure 8, reveals a tendency for series resistance to decrease with increasing temperature, reflecting the classic thermal behavior of electrochemical materials. This can be explained by a reduction in the cell's internal resistivity at high temperatures, facilitating charge transport. However, it is also observed that, for each given temperature, the resistance values obtained in charge and discharge are identical. This symmetrical behavior suggests the absence of any significant hysteresis effect on series resistance under the considered experimental conditions.

## V. CONCLUSION AND FUTURE WORK

The analysis of the experimental curves for series resistance and capacity, expressed in ampere-hours (Ah), clearly and unambiguously demonstrates the significant impact of the temperature on the electrical behavior of the battery. In particular, it is observed that at low temperatures, the battery's performance deteriorates considerably. This degradation is reflected in a sharp increase in internal resistance, indicating a reduction in ionic conductivity within the electrolyte, as well as a substantial decrease in the available capacity. In fact, under such conditions, the measured capacity remains well below the nominal value specified by the manufacturer, failing to reach even half of it. These findings confirm that low temperatures directly affect the battery's internal electrochemical processes, thereby limiting its energy efficiency and its ability to deliver adequate current during operation. Consequently, these results highlight the critical importance of accounting for temperature effects in the modeling, thermal management, and optimal operation of electrochemical energy storage systems.

## REFERENCES


[1] H. A. Gabbar, M. R. Abdussami, and Md. I. Adham, "Optimal Planning of Nuclear-Renewable Micro-Hybrid Energy System by Particle Swarm Optimization," *IEEE Access*, vol. 8, pp. 181049–181073, 2020, doi: 10.1109/ACCESS.2020.3027524.

[2] L. Apa, L. D'Alvia, Z. Del Prete, and E. Rizzuto, "A Characterization of the Uncertainties Associated With an Automated System for the Study of Lithium-Ion Cells: A Case-Study of a Domestic Grid 24-h Scenario," *IEEE Trans. Instrum. Meas.*, vol. 73, pp. 1–11, 2024, doi: 10.1109/TIM.2024.3476559.

[3] F. Ricco Galluzzo *et al.*, "Electrical Characterization and Modeling of an Innovative Acid/Base Flow Battery," *IEEE Access*, vol. 12, pp. 185200–185211, 2024, doi: 10.1109/ACCESS.2024.3512994.

[4] K. Li, F. Wei, K. J. Tseng, and B.-H. Soong, "A Practical Lithium-Ion Battery Model for State of Energy and Voltage Responses Prediction Incorporating Temperature and Ageing Effects," *IEEE Trans. Ind. Electron.*, vol. 65, no. 8, pp. 6696–6708, Aug. 2018, doi: 10.1109/TIE.2017.2779411.

[5] Y. Wang, H. Li, P. He, E. Hosono, and H. Zhou, "Nano active materials for lithium-ion batteries," *Nanoscale*, vol. 2, no. 8, pp. 1294–1305, Aug. 2010, doi: 10.1039/C0NR00068J.

[6] H. Sharma, S. Sharma, and P. K. Mishra, "A critical review of recent progress on lithium ion batteries: Challenges, applications, and future prospects," *Microchem. J.*, vol. 212, p. 113494, May 2025, doi: 10.1016/j.microc.2025.113494.

[7] R. Kumar and K. Das, "Lithium battery prognostics and health management for electric vehicle application – A perspective review," *Sustain. Energy Technol. Assess.*, vol. 65, p. 103766, May 2024, doi: 10.1016/j.seta.2024.103766.

[8] S. Ma *et al.*, "Temperature effect and thermal impact in lithium-ion batteries: A review," *Prog. Nat. Sci. Mater. Int.*, vol. 28, no. 6, pp. 653–666, Dec. 2018, doi: 10.1016/j.pnsc.2018.11.002.

[9] J. S. Menye, M.-B. Camara, and B. Dakyo, "Lithium Battery Degradation and Failure Mechanisms: A State-of-the-Art Review," *Energies*, vol. 18, no. 2, p. 342, Jan. 2025, doi: 10.3390/en18020342.

[10] Y. Yue *et al.*, "Effects of temperature on the ohmic internal resistance and energy loss of Lithium-ion batteries under millisecond pulse discharge," *J. Phys. Conf. Ser.*, vol. 2301, no. 1, p. 012014, July 2022, doi: 10.1088/1742-6596/2301/1/012014.

[11] K. Bellache, M. B. Camara, B. Dakyo, and S. Ramasamy, "Aging Characterization of Lithium Iron Phosphate Batteries Considering Temperature and Direct Current Undulations as Degrading Factors," *IEEE Trans. Ind. Electron.*, vol. 68, no. 10, pp. 9696–9706, Oct. 2021, doi: 10.1109/TIE.2020.3020021.

[12] S. Hossain, X. Kang, and S. Shrestha, "Effects of Temperature on Internal Resistances of Lithium-Ion Batteries," *J. Energy Resour. Technol.*, vol. 137, p. 031901, May 2015, doi: 10.1115/1.4028698.

[13] S. Lv, X. Wang, W. Lu, Z. Jiaqiao, and H. Ni, "The Influence of Temperature on the Capacity of Lithium Ion Batteries with Different Anodes," *Energies*, vol. 15, p. 60, Dec. 2021, doi: 10.3390/en15010060.

[14] B. Kosseila, M. B. Camara, and B. Dakyo, *Characterization and Electric Behavior Modeling of Lithium- Battery using Temporal Approach for Parameters Computing*. 2018, p. 1335. doi: 10.1109/ICRERA.2018.8566742.

[15] Z. Ling *et al.*, "Review on thermal management systems using phase change materials for electronic components, Li-ion batteries and photovoltaic modules," *Renew. Sustain. Energy Rev.*, vol. 31, pp. 427–438, Mar. 2014, doi: 10.1016/j.rser.2013.12.017.

[16] T. Mesbahi, N. Rizoug, P. Bartholomeus, R. Sadoun, F. Khenfri, and P. Le Moigne, "Dynamic Model of Li-Ion Batteries Incorporating Electrothermal and Ageing Aspects for Electric Vehicle Applications," *IEEE Trans. Ind. Electron.*, vol. 65, no. 2, pp. 1298–1305, Feb. 2018, doi: 10.1109/TIE.2017.2714118.

[17] P. Pillai, J. Nguyen, and B. Balasingam, "Performance Analysis of Empirical Open-Circuit Voltage Modeling in Lithium-Ion Batteries, Part-2: Data Collection Procedure," *IEEE Trans. Transp. Electrification*, vol. 11, pp. 153-162, Jan. 2024, doi: 10.1109/TTE.2024.3386910.